Anal. Chem. **2010,** *82,* 9566–9572

Highly Sensitive Electrogenerated Chemiluminescence Biosensor in Profiling Protein Kinase Activity and Inhibition Using Gold Nanoparticle as Signal Transduction Probes

Shoujiang Xu,[†,‡] Yang Liu,[*,†] Taihong Wang,[‡] and Jinghong Li[*,†]

Department of Chemistry, Key Lab of Bioorganic Phosphorus Chemistry and Chemical Biology, Tsinghua University, Beijing 100084, China, and Key Laboratory for Micro-Nano Optoelectronic Devices of Ministry of Education and State Key Laboratory for Chemo/Biosensing and Chemometrics, Hunan University, Changsha 410082, China

A novel electrogenerated chemiluminescence (ECL) biosensor using gold nanoparticles as signal transduction probes was described for the detection of kinase activity. The gold nanoparticles were specifically conjugated to the thiophosphate group after the phosphorylation process in the presence of adenosine 59-[c-thio] triphosphate (ATP-s) cosubstrate. Due to its good conductivity, large surface area, and excellent electroactivity to luminol oxidization, the gold nanoparticles extremely amplified the ECL signal of luminol, offering a highly sensitive ECL biosensor for kinase activity detection. Protein kinase A (PKA), an important enzyme in regulation of glycogen, sugar, and lipid metabolism in the human body, was used as a model to confirm the proof-of-concept strategy. The as-proposed biosensor presented high sensitivity, low detection limit of 0.07 U mL^{-1}, wide linear range (from 0.07 to 32 U mL^{-1}), and excellent stability. Moreover, this biosensor can also be used for quantitative analysis of kinase inhibition. On the basis of the inhibitor concentration dependent ECL signal, the half-maximal inhibition value IC_{50} of ellagic acid, a PKA inhibitor, was estimated, which was in agreement with those characterized with the conventional kinase assay. While nearly no ECL signal change can be observed in the presence of Tyrphostin AG1478, a tyrosine kinase inhibitor, but not PKA inhibitor, shows its excellent performance in kinase inhibitor screening. The simple and sensitive biosensor is promising in developing a high-through assay of in vitro kinase activity and inhibitor screening for clinic diagnostic and drug development.

Protein phosphorylation by kinase plays a critical regulatory role in a majority of biological processes including metabolism, cell growth, cellular signal communications, and survival differentiation.[1−3] Over 500 protein kinase genes are contained in human genes, and they constitute about 2% of all human genes. Up to 30% of all human proteins are modified by kinase activity, and kinases regulate the majority of cellular pathways, especially those involved in signal transduction. Since aberrant protein phosphorylation states and kinase activity are linked with many common diseases, such as various cancer[4,5] and Alzheimer's diseases,[6,7] accurate identification of protein kinase activity and their potential inhibitors is not only valuable to provide insights regarding the fundamental biochemical process of diseases but also essential to the protein kinase-targeted drug discovery and molecular-target therapies.

In these years, kinase assays based on electrochemical methods have been developed quickly. Compared to other methods such as radioactive,[8] fluorescence[9−12] and surface-plasma resonance[13,14] analysis systems, electrochemical methods are simple, cost-effective, and sensitive. A lot of electrochemical biosensors have been designed lately for the detection of kinase activity by measuring the current and charge responses of redox

* To whom corresponding should be addressed. Phone: 86-10-62795290. Fax: 86-10-62771149. E-mail: liu-yang@mail.tsinghua.edu.cn (Y.L.); jhli@mail.tsinghua.edu.cn (J.L.).

† Tsinghua University.

‡ Hunan University.

(1) Manning, G.; Whyte, D. B.; Martinez, R.; Hunter, T.; Sudarsanam, S. *Science* **2002**, *298*, 1912–1934.
(2) Cohen, P. *Nat. Cell Biol.* **2002**, *4*, E127−E130.
(3) Kalume, D. E.; Molina, H.; Pandey, A. *Curr. Opin. Chem. Biol.* **2003**, *7*, 64–69.
(4) Nicholson, R. I.; Gee, J. M. W.; Harper, M. E. *Eur. J. Cancer* **2001**, *37*, 9–15.
(5) Schlessinger, J. *Cell* **2000**, *103*, 211–225.
(6) Flajolet, M.; He, G.; Heiman, M.; Lin, A.; Nairn, A. C.; Greengard, P. *Proc. Natl. Acad. Sci. U.S.A.* **2007**, *104*, 4159–4164.
(7) Hanger, D. P.; Byers, H. L.; Wray, S.; Leung, K.-Y.; Saxton, M. J.; Seereeam, A.; Reynolds, C. H.; Ward, M. A.; Anderton, B. H. *J. Biol. Chem.* **2007**, *282*, 23645–23654.
(8) Houseman, B. T.; Huh, J. H.; Kron, S. J.; Mrksich, M. *Nat. Biotechnol.* **2002**, *20*, 270–274.
(9) Rothman, D. M.; Shults, M. D.; Imperiali, B. *Trends Cell Biol.* **2005**, *15*, 502–510.
(10) Hyun-Woo, R.; Seung Hwan, L.; Ik-Soo, S.; Jung, C.; Hun, P.; Kyungja, H.; Tai Hyun, P.; Jong-In, H. *Angew. Chem., Int. Ed.* **2010**, *49*, 4919–4923.
(11) Sun, H.; Low, K. E.; Woo, S.; Noble, R. L.; Graham, R. J.; Connaughton, S. S.; Gee, M. A.; Lee, L. G. *Anal. Chem.* **2005**, *77*, 2043–2049.
(12) Agnes, R. S.; Jernigan, F.; Shell, J. R.; Sharma, V.; Lawrence, D. S. *J. Am. Chem. Soc.* **2010**, *132*, 6075–6080.
(13) Yoshida, T.; Sato, M.; Ozawa, T.; Umezawa, Y. *Anal. Chem.* **1999**, *71*, 6–11.
(14) Stenlund, P.; Frostell-Karlsson, A.; Karlsson, O. P. *Anal. Biochem.* **2006**, *353*, 217–225.

10.1021/ac102296g
Published on Web 10/26/2010

probes conjugated during the phosphorylation processes.[15−21] Kerman and co-workers reported the quantitative measurements of phosphorylation reactions based on oxidation current of tyrosine[15] and ferrocene.[16] To simplify the detection procedure, a gold nanoparticle labeled phosphorylation process for the kinase assay was also designed in this group by measuring the redox currents of gold nanoparticles, yet a low sensitivity was achieved.[22] Recently, Willner reported a novel method for kinase activity analysis by monitoring the voltammetric response of Ag^+ ions associated with the phosphorylated product.[20] To amplify the electrochemical response and improve the sensitivity, a TiO_2-assisted silver enhanced electrochemical biosensor for kinase activity profiling was developed by the specific binding of phosphate groups with TiO_2 nanoparticles.[18] Recently, a DNA-based strategy was also described by the chronocoulometric response of $Ru(NH_3)_6^{3+}$ absorbed on the DNA−gold nanoparticles that linked with the phosphorylated peptide by Zr^{4+}.[21] Despite the improvement of these methods, sophisticated procedures of electroactive labeling such as DNA functionalization of gold nanoparticles, deposition of metallic probes, etc. are needed, and sometimes, the performances such as linear range, sensitivity, etc. were also limited. Therefore, it is still a challenge in developing sensitive, rapid, accurate, and simple methods for the profiling of kinase activity and inhibition.

Electrogenerated chemiluminescence (ECL) is a light emission process in a redox reaction of electrogenerated reactants, which combines the electrochemical and luminescent techniques.[23−26] Compared to the conventional electrochemical methods and luminescence techniques, the ECL technique not only shows high sensitivity and wide dynamic concentration response range but also is potential and spatial controlled. ECL biosensor is a powerful device for ultrasensitive biomolecule detection and quantification by combining the selectivity of the biological recognition elements and the sensitivity of ECL technique and is widely used in immunoassay,[27−30] DNA analysis,[31−35] environmental detection, and clinic diagnostics.[36−39] In spite of its excellent properties, few studies have been conducted concerning the detection of kinase activity and inhibition by ECL methods.[40]

Owing to their good biocompatibility, fascinating electrocatalytic activity, large surface area, excellent conductivity, and stability, gold nanoparticles received much attention in electrochemistry, biosensing, imaging and, so on.[41−43] Gold nanoparticles have been widely used in designing ECL biosenesors.[26,44,45] The performances of ECL biosensors are heavily dependent on the signal-transduction ways. Optimized and suitable labels will offer the possibility of substantial signal amplification. Generally, the gold nanoparticle-based ECL biosensors utilize gold nanoparticles for the modification of the substrate electrodes,[44,46] which provide large electrode/solution interface area and also facilitate the electron transfer between the ECL labels and the electrodes, thus affording the possibility of performance improvement. In an alternative way, gold nanoparticles can also work as carriers of conventional active labels[33,34] such as enzymes and electroactive species and, thus, afford substantial ECL signal amplification.

In this work, the proof-of-concept of a novel ECL biosensor for the kinase activity and inhibition analysis using gold nanoparticle as a sensitive signal transduction probe was demonstrated. Using protein kinase A (PKA) as a model kinase, the gold nanoparticles were assembled onto the electrode based on the introduction of thiol group during the kinase catalyzed-phosphorylation process in the presence of Adenosin 59-[c-thio] triphosphate (ATP-s). The assembled gold nanoparticles then mediated the ECL reaction of ECL indicators, extremely amplifying the ECL signal and supplying a sensitive strategy for the identification of kinase activity. Here, luminol was chosen as the ECL indicator because of its low oxidation potential, inexpensive reagent consumption, and the high emission yields. To the best of our knowledge, it is the first time for kinase activity analysis based on ECL methods using gold nanoparticle as a sensitive signal transduction probe. This strategy provides a simple, sensitive, selective, and universal platform for kinase activity assay and inhibitor screening.

EXPERIMENTAL SECTION

Materials and Reagents. Protein kinase A (PKA, catalytic subunit from recombinant *E. coli* strain) was obtained from Promega (America). Cysteine-terminated kemptide (H−CLRRASLG−OH) was purchased from GL Biochem (Shanghai, China). Adenosine 5′-

(15) Kerman, K.; Vestergaard, M. d.; Tamiya, E. *Anal. Chem.* **2007**, *79*, 6881–6885.
(16) Kerman, K.; Song, H.; Duncan, J. S.; Litchfield, D. W.; Kraatz, H.-B. *Anal. Chem.* **2008**, *80*, 9395–9401.
(17) Kerman, K.; Kraatz, H.-B. *Biosens. Bioelectron.* **2009**, *24*, 1484–1489.
(18) Ji, J.; Yang, H.; Liu, Y.; Chen, H.; Kong, J.; Liu, B. *Chem. Commun.* **2009**, 1508–1510.
(19) Kerman, K.; Kraatz, H.-B. *Chem. Commun.* **2007**, 5019–5021.
(20) Wieckowska, A.; Li, D.; Gill, R.; Willner, I. *Chem. Commun.* **2008**, 2376–2378.
(21) Xu, X.; Nie, Z.; Chen, J.; Fu, Y.; Li, W.; Shen, Q.; Yao, S. *Chem. Commun.* **2009**, 6946–6948.
(22) Kerman, K.; Chikae, M.; Yamamura, S.; Tamiya, E. *Anal. Chim. Acta* **2007**, *588*, 26–33.
(23) Richter, M. M. *Chem. Rev.* **2004**, *104*, 3003–3036.
(24) Marquette, C. A.; Thomas, D.; Degiuli, A.; Blum, L. J. *Anal. Bioanal. Chem.* **2003**, *377*, 922–928.
(25) Marquette, C. A.; Blum, L. J. *Anal. Bioanal. Chem.* **2009**, *390*, 155–168.
(26) Bertoncello, P.; Forster, R. J. *Biosens. Bioelectron.* **2009**, *24*, 3191–3200.
(27) Ala-Kleme, T.; Makinen, P.; Ylinen, T.; Vare, L.; Kulmala, S.; Ihalainen, P.; Peltonen, J. *Anal. Chem.* **2006**, *78*, 82–88.
(28) Jie, G. F.; Zhang, J. J.; Wang, D. C.; Cheng, C.; Chen, H. Y.; Zhu, J. J. *Anal. Chem.* **2008**, *80*, 4033–4039.
(29) Marschall, A.; Finke, A.; Raschmenges, J. *Clin. Chem.* **1995**, *41*, S80–S80.
(30) Liu, X.; Ju, H. X. *Anal. Chem.* **2008**, *80*, 5377–5382.
(31) Zhang, L.; Li, D.; Meng, W.; Huang, Q.; Su, Y.; Wang, L.; Song, S.; Fan, C. *Biosens. Bioelectron.* **2009**, *25*, 368–372.
(32) Li, Y.; Qi, H. L.; Peng, Y.; Yang, J.; Zhang, C. X. *Electrochem. Commun.* **2007**, *9*, 2571–2575.
(33) Duan, R.; Zhou, X.; Xing, D. *Anal. Chem.* **2010**, *82*, 3099–3103.
(34) Pinijsuwan, S.; Rijiravanich, P.; Somasundrum, M.; Surareungchai, W. *Anal. Chem.* **2008**, *80*, 6779–6784.
(35) Hu, L.; Bian, Z.; Li, H.; Han, S.; Yuan, Y.; Gao, L.; Xu, G. *Anal. Chem.* **2009**, *81*, 9807–9811.
(36) Miao, W.; Bard, A. J. *Anal. Chem.* **2004**, *76*, 7109–7113.
(37) Fahnrich, K. A.; Pravda, M.; Guilbault, G. G. *Talanta* **2001**, *54*, 531–559.
(38) Lu, Y. M.; Young, J.; Meng, Y. G. *Curr. Opin. Pharm.* **2007**, *7*, 541–546.
(39) Wang, Y.; Lu, J.; Tang, L.; Chang, H.; Li, J. *Anal. Chem.* **2009**, *81*, 9710–9715.
(40) Xiao, S. H.; Farrelly, E.; Anzola, J.; Crawford, D.; Jiao, X.; Liu, J.; Ayres, M.; Li, S.; Huang, L.; Sharma, R.; Kayser, F.; Wesche, H.; Young, S. W. *Anal. Biochem.* **2007**, *367*, 179–189.
(41) Liu, G.; Lin, Y. *Talanta* **2007**, *74*, 308–317.
(42) Rusling, J. F.; Sotzing, G.; Papadimitrakopoulosa, F. *Bioelectrochem.* **2009**, *76*, 189–194.
(43) Wang, J. In *Perspectives in Bioanalysis*; Palecek, E., Scheller, F., Wang, J., Eds.; Elsevier: 2005; Vol. 1, pp 369−384.
(44) Cui, H.; Xu, Y.; Zhang, Z. F. *Anal. Chem.* **2004**, *76*, 4002–4010.
(45) Zhou, X.; Xing, D.; Zhu, D.; Jia, L. *Anal. Chem.* **2009**, *81*, 255–261.
(46) Jie, G. F.; Liu, P.; Zhang, S. S. *Chem. Commun.* , *46*, 1323–1325.

Scheme 1. Schematic Representation of ECL Strategy for Kinase Activity Detection Using Gold Nanoparticles as Signal Transduction Probes

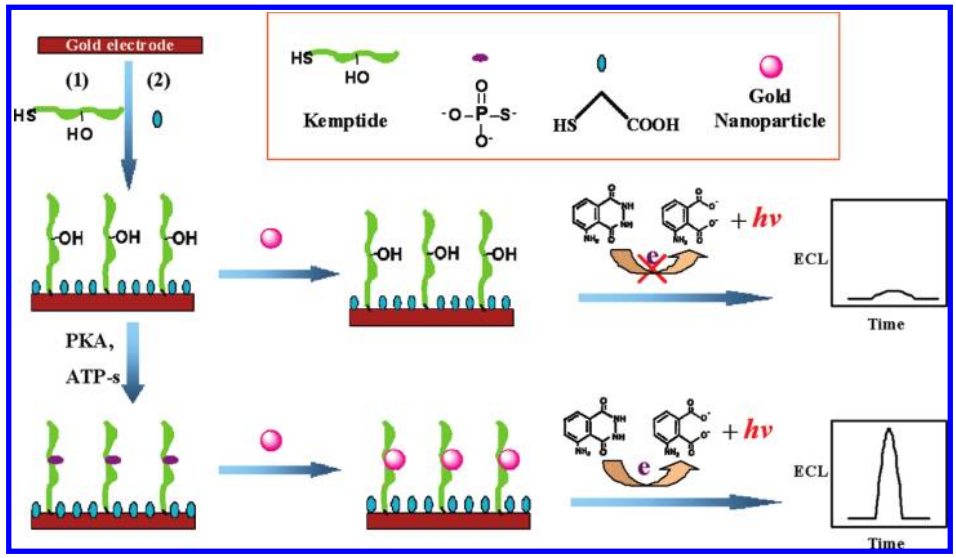

[γ-thio] triphosphate tetra-lithium salt (ATP-γ-s), 4,4′,5,5′,6,6′-hexahydroxydiphenic acid 2,6,2′,6′-dilactone (Ellagic acid), *N*-(3-chlorophenyl)-6,7-dimethoxy-4-quinazolinamine (Tyrphostin AG 1478), and luminol were purchased from Sigma. A 1.0×10^{-2} M stock solution of luminol was prepared by dissolving luminol in 0.1 mol/L sodium hydroxide solution. The preparation of gold nanoparticle colloidal solution and instrument characterizations are described in Supporting Information.

Assembly and Phosphorylation of Kemptide on Gold Electrode. A gold electrode (diameter of 2 mm) was polished carefully first with 1.0, 0.3, and 0.05 μm α-Al_2O_3 powder on fine abrasive paper and rinsed with water. Then, the electrode was washed ultrasonically with ethanol and water. Prior to immobilization of kemptide, the gold electrode was scanned in 0.5 M H_2SO_4 between -0.2 and 1.55 V (vs Ag/AgCl) until a reproducible cyclic voltammogram was obtained. After cleaning, the gold electrode was immersed into a PBS (0.05 M, pH 7.5) solution containing 500 μM cysteine terminated kemptide at room temperature in darkness for 15 h. The resulting kemptide modified electrodes were rinsed thoroughly with blank PBS, followed by immersion in 2 mM mercaptoacetic acid solution for 1 h at ambient temperature to block the nonspecific binding sites on the electrode. Finally, the peptide assembled electrodes were rinsed with blank PBS and ready for phosphorylation. PKA-catalyzed phosphorylation was performed by incubating the kemptide modified gold electrode into an assay buffer solution (40 mM Tris−HCl and 20 mM $MgCl_2$, pH 7.4) containing a desired amount of PKA and ATP-γ-S at 30 °C for 1 h. In the inhibition experiment, a desired concentration of inhibitors was also contained in the assay buffer solutions, and the procedures were similar as above.

ECL Characterization of PKA-Catalyzed Phosphorylation Reaction and Kinase Activity Detection. The phosphorylated kemptide modified electrode was immersed into a 2 mL colloidal gold nanoparticle solution at room temperature for 30 min. Gold nanoparticles were then adsorbed onto the phosphorylated electrode surface through the gold−sulfur bond. After washing to remove the nonspecific gold nanoparticles, the resulting electrode was characterized by an ECL technique in a luminol solution. The electrolyte solution was prepared by diluting the luminol stock with PBS (0.1 M, pH 10.5) with a final concentration of luminol at 100 μM. The modified gold electrode acted as working electrodes, and a Ag/AgCl with saturated KCl solution and platinum wire was used as the reference electrode and counter electrode, respectively.

RESULTS AND DISCUSSION

ECL Strategy for Kinase Activity Detection Using Gold Nanoparticles as Signal Transduction Probes. The developed ECL strategy in profiling the kinase activity is described in Scheme 1. The cysteine-terminated kemptides were immobilized on the gold electrode through the Au−S bond to form a dense assemble layer. To decrease the nonspecific adsorption, mercaptoacetic acid was further assembled on the blank binding sites. After the phosphorylation reaction in the presence of PKA using ATP-s as the cosubstrate, thiolated substrate peptides were introduced on the electrode surface. The high affinity between gold nanoparticles and the thiophosphate group causes the assembly of gold nanoparticles on the substrate peptide. The gold nanoparticles extremely amplified the ECL signal of luminol due to their excellent electrocatalytic activity toward the luminol ECL reaction,[44] good conductivity, and large surface area that facilitates the electron transfer on the electrode interface. As a comparison, nearly no gold nanoparticle was adsorbed on the peptide modified electrode in the absence of PKA. The dense and insulated peptide layer also isolated the electrode and solution and inhibited the electron transfer between luminol and electrode; thus, a much weaker ECL response was deserved in the absence of PKA. Moreover, more thiophosphate groups were obtained on the electrode at higher activity of kinase, and thus, a higher density of gold nanoparticles on the electrode and stronger ECL response were achieved, offering a quantitative readout of kinase activity.

Fabrication and Characterization of the Biosensors. In the experiments, kemptide was directly immobilized on the gold electrode surface via the Au−S bond between the end cysteine in kemptide sequence and gold electrode (Scheme 1a). The amount of kemptide assembled on the gold electrode can be quantitatively characterized based on the adsorption of sulfur

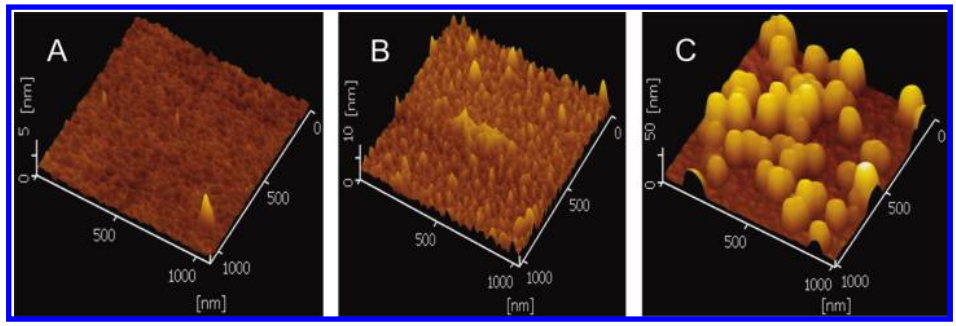

Figure 1. AFM images of (A) bare gold electrode, (B) cysteine-terminated kemptide modified gold electrode, and (C) gold nanoparticles assembled after the thiophosphorylation by PKA with ATP-s as cosubstrate on the gold electrode.

atoms. Reductive desorption by voltammetry is a widely used tool to quantitatively characterize the surface adsorption of sulfur atoms. The well-defined reduction peak (Figure S2 in the Supporting Information) is responsible for the desorption of cysteine-determinated kemptide on the gold electrode. The surface coverage of kemptide on the gold electrode was calculated to be 3.2×10^{-11} mol cm^{-2} as ascertained from the first reduction peak in the stripping voltammetry based on one-electron reduction. The phosphorylation of kemptide was confirmed by FT-IR spectra (Figure S3 in Supporting Information). After the PKA-catalyzed reaction in the presence of S-ATP, the thiolated phosphate groups were transferred to the serine residue of kemptide on the electrode surface. Besides the characteristic peaks of kemptide (curve a, Figure S3 in the Supporting Information), two peaks located at 1205 and 1137 cm^{-1} appeared (curve b, Figure S3 in the Supporting Information) and were ascribed to the stretching vibration of P═O and C−O−P bonds in the phosphorylated kemptide, respectively, indicating the accomplishment of kemptide phosphorylation.

The atomic force microscopy (AFM) technique was employed to characterize the assembling processes of gold nanoparticle during the phosphorylation procedure of kemptide. Figure 1A shows the image of the bare gold substrate. A smooth and homogeneous surface appeared. After the modification of cysteine-terminated kemptide, plenty of hillocks with a height of ca. 2.5 nm are presented (Figure 1B). The fact suggests that kemptide is successfully assembled onto the gold electrode. Figure 1C illustrates the graph of a gold nanoparticle assembled gold electrode after the thiophosphorylation by PKA with ATP-s as cosubstrate. A large number of islandlike prominences appeared, and it was clearly distinguished from that in Figure 1B before gold nanoparticles assembly. The height of the prominence in the AFM image was ca. 35 nm and was similar to the size of the gold nanoparticle obtained from TEM, confirming the assembly of gold nanoparticles on the modified electrode.

A cyclic voltammogram (CV) was also used to evaluate the assembly processes by monitoring the electron transfer ability tunneling through the barrier layer between the electroactive probes and gold electrode. Figure 2A shows the CV curves characterizing the step-by-step buildup process of the modified gold electrode using $Fe(CN)_6^{4-/3-}$ as electroactive probe couple. As can be seen, a couple of quasi-reversible redox peaks of the probes were obtained in the bare gold electrode (curve a). When the gold electrode was first treated with kemptide, the monolayer of kemptide on the gold electrode led to a decrease of peak current (curve b). The fact is ascribed to the electron

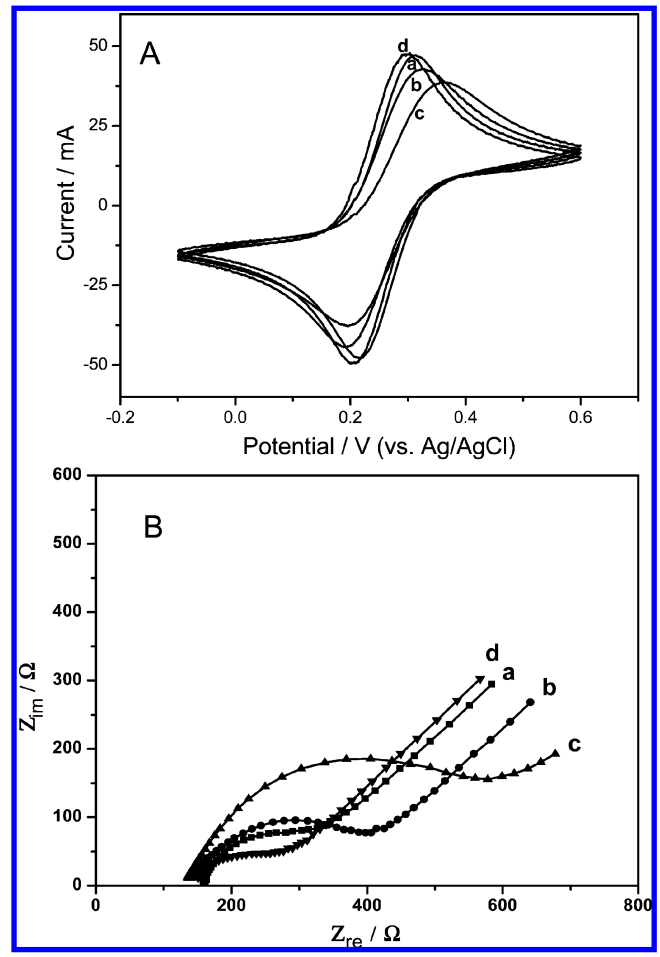

Figure 2. Cyclic voltammograms (A) and electrochemical impedance spectra (B) of bare gold (curve a), kemptide modified gold electrode (curve b), phosphorylated kemptide modified electrode before (curve c), and after (curve d) the assembly of gold nanoparticles in 0.1 M KCl solution with 5 mM $[Fe(CN)_6]^{3-/4-}$ electroactive probes, respectively. Scan rate is 100 mV s^{-1}. The frequency range is between 0.1 and 10^5 Hz with signal amptitude of 5 mV in panel B.

inert feature of kemptide which partially blocks the electron transfer and mass transfer of $Fe(CN)_6^{4-/3-}$ ions on the surface of gold electrode. After the thiophosphorylation by PKA, the peak current in the CV decreased further, and the potential gap between the anodic and cathodic peaks became wider (curve c). It is reasoned that the replacement of hydroxide group by phosphate group increases the negative charge density of kemptide and hinders the electron transfer at the electrode interface. In addition, the large size of phosphate

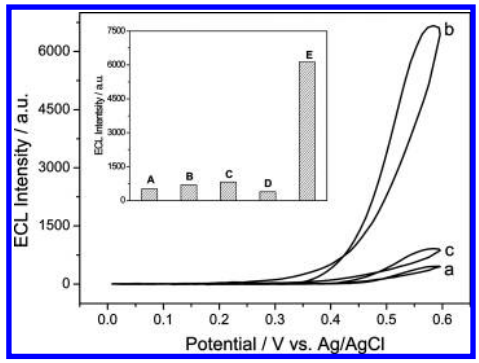

Figure 3. ECL−potential curves of phosphorylated kemptide modified electrode before (a) and after (b) the treatment with gold nanoparticle colloidal solution. (c) The ECL−potential curve of the kemptide modified electrode without phosphorylation after the treatment with gold nanoparticle colloidal solution. The inset shows the ECL intensity of the bare gold electrode (A, B), kemptide modified electrode (C), and phosphorylated kemptide modified electrode (D, E) before (A, D) and after (B, C, E) treatment with gold colloidal solution, respectively. The protein kinase A assay was carried out in a Tris−HCl buffer solution (40 mM, pH 7.4) containing 20 mM $MgCl_2$, 100 μM ATP-s, and 55 U/mL PKA. The ECL measurements were performed in a 0.1 M PBS (pH 10.5) containing 100 μM luminol at a scan rate of 100 mV s^{-1}. The voltage of PMT was maintained at 600 V.

groups also inhibited the mass transport of $Fe(CN)_6^{4-/3-}$ probes toward the modified electrode. When gold nanoparticles were assembled on the modified electrode, an obvious increase in the amperometric response was found (curve d), and the peak current after the assembly of gold nanoparticles was even larger than that of bare gold. This phenomena was also confirmed by electrochemical impedance spectra (EIS) as shown in Figure 2B. In the Nyquist plot, the diameter of the semicircle at higher frequency range is equal to the electron transfer resistance, which represents the electron transfer kinetics of the electroactive probes at the electrode interface. It was clear that the diameter of semicircle after the assembly of kemptide (curve b) was larger than that of bare gold electrode (curve a), indicating an increase of the electron transfer resistance after the assembly of kemptide on the gold electrode. The electron transfer resistance increased further after phosphorylation (curve c) and decreased after the assembly of gold nanoparticles (curve d). The phenomena are consistent to those in CV. The facts elucidate that the gold nanoparticles can largely reduce the electron transfer resistance of the redox probes at the electrode interface even if an inert block layer was assembled on the electrode.

ECL Behavior of the Biosensor. Figure 3 shows the ECL emission as a function of potential on the thiophosphorylated kemptide modified electrode before (a) and after (b) treatment with gold nanoparticles in a solution containing 50 mM luminol. There is an ECL peak at about 0.55 V in both curves, resulting from the ECL reaction of luminol.[44] As it is shown, phosphorylated kemptide modified electrode exhibits much weaker ECL signal. However, when the phosphorylated kemptide modified electrode was immersed into the gold nanoparticle colloidal solution and the gold nanoparticles were assembled onto the modified electrode as shown above, a strong ECL peak at 0.55 V was observed, resulting from the ECL reaction of luminol. The emission intensity of luminol after the assembly of gold nanoparticles is nearly ten times larger than that of the modified electrode without gold nanoparticles. In the presence of oxygen, the ECL reaction of luminol can be described as electrode reactions which follows by chemical reactions.[44]

$$LH^- - e^- \rightarrow LH^\bullet \rightarrow L^{\bullet -} + H^+$$

$$L^{\bullet -} + O_2 \rightarrow O_2^{\bullet -} + L$$

$$L^{\bullet -} + O_2^{\bullet -} \rightarrow LO_2^{2-}$$

$$LO_2^{2-} \rightarrow AP^{2-*} + N_2$$

$$AP^{2-*} \rightarrow AP^{2-} + h\nu\,(425\,nm)$$

Where LH^- is the deprotonated luminol and AP^{2-*} is the excited state product, it is noted that the gold nanoparticles will not only increase the interface area of the modified electrode to capture more active molecules but also facilitate the electron transfer at the electrode interface and catalyze the ECL process of luminol in both electrode and chemical reactions. Thus, the gold nanoparticles can mediate the ECL reaction even at a low content, implying highly efficient ECL signal amplification. In addition, the ECL behavior of the kemptide modified electrode without phosphorylation but treated with gold nanoparticle colloidal solution was also measured as shown in curve c (Figure 3). Like that of the kemptide modified electrode before phosphorylation, a much weaker ECL peak was observed at 0.5 V. The results reveal that gold nanoparticles can be used as a sensitive signal transduction probe to characterize the phosphorylation processes. At higher kinase activity, there are more gold nanoparticles on the electrode giving a larger interface area, faster electron transfer at the electrode interface, and higher electrocatalytic efficiency to the luminol ECL reaction. Thus, the as-designed ECL biosensor can be used for kinase activity characterization.

A series of control experiments were also conducted by the luminol ECL measurement. As shown in the inset of Figure 3, the bare gold electrodes both before (A) and after (B) treatment of gold nanoparticles presented quite weak signals. The ECL signals on the kemptide modified electrode with treatment of gold nanoparticles were also weak but showed a slight increase as compared to the bare gold electrode. These responses could arise from the nonspecific adsorption of gold nanoparticles by electrostatic interaction. However, the ECL signal intensities for all above cases were much weaker than that of the phosphorylated kamptide modified electrode (E). The results confirmed that the phosphorylation process as well as the PKA activity could be identified through the strategy of gold nanoparticle mediated ECL amplification of luminol. We reason these tactics possess several unprecedented advantages. First, the direct assembly of gold nanoparticles avoids the time-consuming and complicated experimental procedures of voltammetric analysis and surface modification of gold nanoparticles. In the second, the low working potential and the absence of coreactants such as H_2O_2, $Na_2S_2O_3$, etc. in the luminol ECL reaction also prohibit the perturbation to the surface attached peptides. Accordingly, the as-proposed strategy provides a simple, sensitive, selective, and universal platform for kinase activity assay and inhibitor screening.

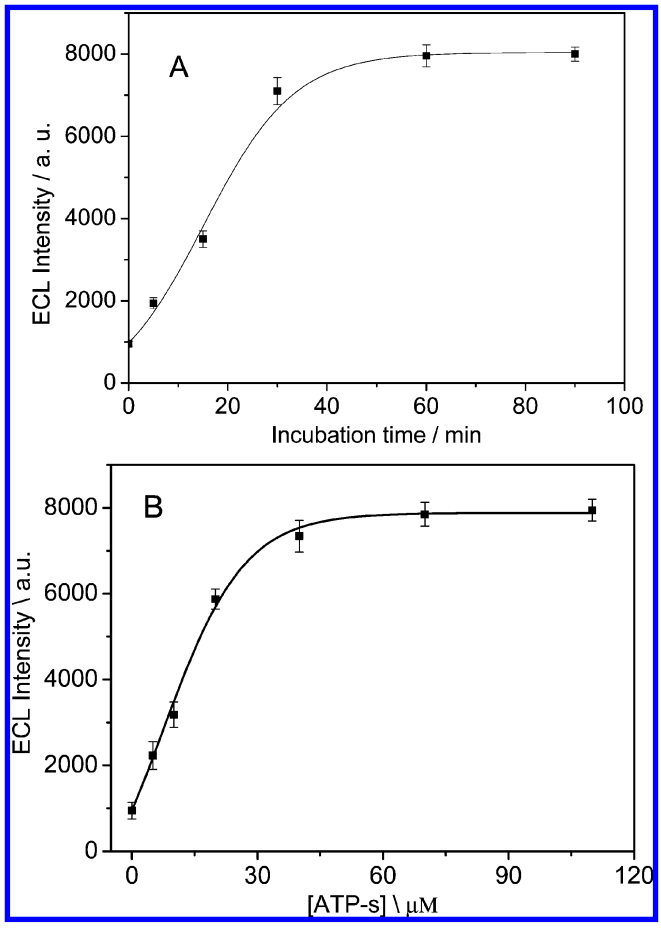

Figure 4. (A) ECL intensity as a function of incubation times in the solution containing PKA and ATP-s. (B) The ECL intensity as a function of the concentration of ATP-s.

Optimization of ECL Detection Conditions. The phosphorylation time is an important parameter for the kinase-catalyzed reaction on the electrode surface. With the increase of the incubation time, the ECL signal of the electrode increased and then reached a plateau in 60 min (Figure 4A), indicating a tendency to complete phosphorylation of kemptide. After that, the increasing time no longer enhanced the ECL intensity. Therefore, the optimal phosphorylation time was 60 min. In addition, the enzyme catalyzed reaction is also sensitive to the temperature. The optimal temperature for the phosphorylation procedure of kemptide by PKA was 30 °C in these experiments (Figure S4 in the Supporting Information).

The nucleotide triphosphate (ATP) offers the phosphate groups during the phosphorylation reaction. As shown in Figure 4B, the ECL intensity of the kemptide modified electrode increased with the increasing concentrations of ATP-s in the presence of PKA of 80 U mL^{-1}. The ECL signal reached a maximal value at the ATP-s concentration of 75 μM and maintained the intensity at higher concentration of ATP-s. The facts manifested that 75 μM ATP-s was sufficient to the phosphorylation reaction catalyzed by PKA. Thus, the optimal concentration of ATP-s was 75 μM.

ECL Measurement of PKA Activity. On the basis of the optimal condition, the activity of protein kinase was evaluated with different concentrations of PKA. When the PKA units increased,

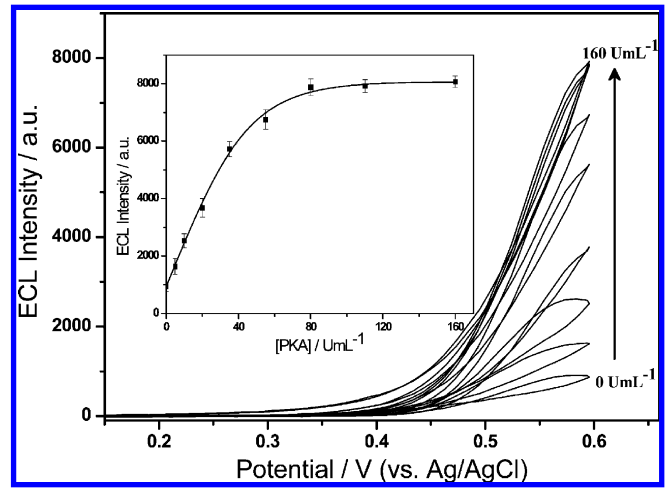

Figure 5. ECL intensity−potential curves with different activity units of PKA. The inset shows the dependence of ECL intensity on the concentration of protein kinase A (PKA). The assays were carried out in a Tris−HCl buffer solution (40 mM, 20 mM $MgCl_2$, pH 7.4), containing 100 μM ATP-s and designated concentrations of PKA. The scan rate is 100 mV/s.

the ECL signal increased accordingly (Figure 5) and reached a saturation value once the concentration of PKA was above 110 U mL^{-1}. The dependence of the ECL response on the PKA concentration is presented in the inset of Figure 5. A linear relationship between ECL signals and the concentrations of PKA was obtained in the range from 0.07 to 35 U mL^{-1}. The detection limit of PKA was 0.07 U mL^{-1} (signal-to-noise ratio of 3), which was lower than that of previous reported electrochemical assays.[18,21,22] The linear relationship can be represented as $I = 1114.18 + 130.97 \times c$ with the correlation coefficient of $R^2 = 0.9963$, where I is the ECL intensity and c is the kinase activity. This demonstrates that the proposed ECL method can be employed for highly sensitive kinase activity detection in a wide concentration range.

Stable and high ECL signals (Figure S5 in the Supporting Information) were observed when the biosensor was successively scanned, which signified that the ECL biosensor possessed excellent potential cycling stability. As it was stated, the redox coreactants such as H_2O_2 were not involved during the ECL reaction. Thus, the damage to the modified electrodes and biomolecules by the coreactants was avoided, supplying a high stability of the ECL biosensor for kinase activity detection. The reproducibility of the ECL biosensor was also studied with intra- and interassay precision. The intraassay precision of the ECL biosensor was evaluated by measuring the one level of PKA activity ten times. The interassay precision was assessed by assaying the same level of PKA activity with ten electrodes. The intra- and the interassay variation coefficients obtained from 75 U mL^{-1} PKA were 4.6% and 5.9%, respectively. Both the intra- and interassays of the as-designed ECL biosensor enunciate acceptable reproducibility.

Kinase Activity Inhibition Evaluation. The gold nanoparticle mediated ECL biosensor was also used to quantitatively evaluate the inhibition of kinase in the presence of small molecule

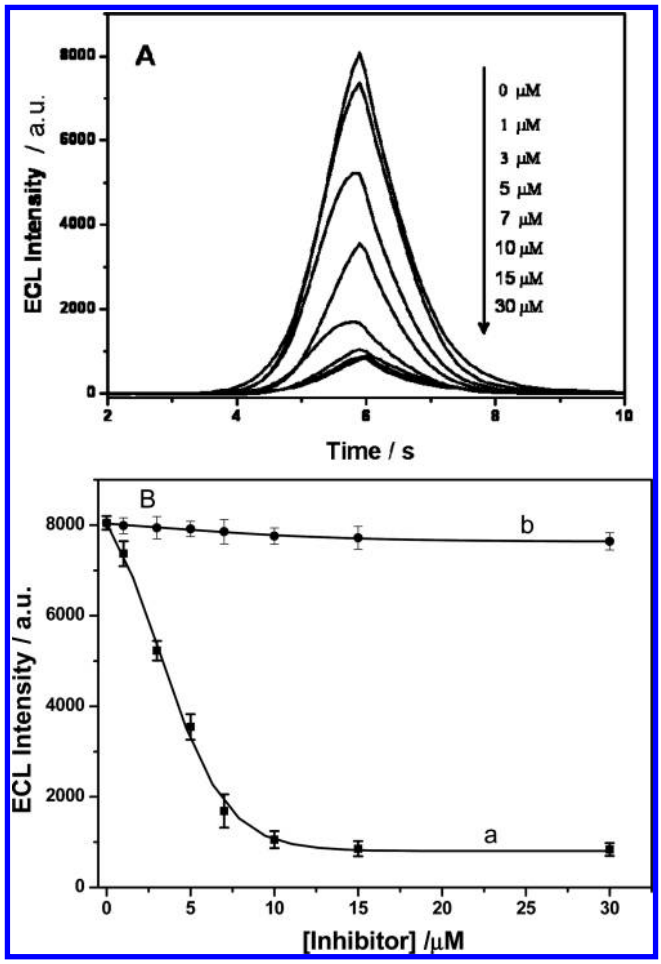

Figure 6. (A) ECL intensity−time behaviors at different concentrations of ellagic acid. (B) The ECL intensity as a function of concentrations of ellagic acid (a) and Tyrphostin AG 1478 (b). The phosphorylation of kemptide was carried out with 80 U mL^{-1} PKA and 75 μM ATP-s. Error bars were obtained from three times parallel experiments.

inhibitors. In the inhibition assay, the PKA activities were evaluated with PKA inhibitors at different concentrations, and the half-maximal inhibition value IC_{50} was calculated. Here, ellagic acid, a cell-permeable and potent antioxidant with antimutagenic and anticarcinogenic properties, was employed as a inhibitor. As shown in Figure 6A, the ECL signal decreased with the increasing concentrations of ellagic acid. Only weak ECL signal was observed with the addition of ellagic acid at 10 μM. Curve a in Figure 6B presents the concentration dependent ECL signals. On the basis of the results, the IC_{50} of ellagic acid was measured to be 3.78 μM, which is in agreement with that reported in the literature obtained with a conventional kinase assay.[47] In addition, Tyrphostin AG 1478, a tyrosine kinase inhibitor but not PKA inhibitor, was also added to evaluate the specificity of the ECL biosensor. The concentration dependent ECL signal is shown in curve b of Figure 6B. As expected, the ECL signals nearly had no change in the presence of the tyrosine kinase inhibitor with a concentration as high as 30 μM, showing its excellent specificity to the kinase inhibitor profiling. These results indicate that the proposed gold nanoparticle mediated ECL strategy is a potential in quantitatively screening the activity of the kinase inhibitors.

(47) Cozza, G.; Bonvini, P.; Zorzi, E.; Poletto, G.; Pagano, M. A.; Sarno, S.; Donella-Deana, A.; Zagotto, G.; Rosolen, A.; Pinna, L. A.; Meggio, F.; Moro, S. *J. Med. Chem.* **2006**, *49*, 2363–2366.

CONCLUSIONS

In conclusion, a novel ECL biosensor using gold nanoparticle as a signal transduction probe has been developed for kinase activity and inhibition assay. The ultrahigh amplification efficiency of gold nanoparticles to the luminol ECL reaction allows the sensitive detection of kinase activity. This strategy provides a simple detection procedure and also avoids the high potential and coreactants such as H_2O_2, $Na_2S_2O_3$, etc. during the ECL measurements. As a result, the as-proposed ECL biosensor offers a highly sensitive strategy for PKA kinase activity monitoring with a low detection limit of 0.07 U/mL, wide linear range, and good stability. Moreover, the proof-of-concept method also shows excellent performance on the accurate and quantitative kinase inhibitor assay, verifying with well-known kinase inhibition systems. The general and robust method can also be ready for other kinase activities and inhibition assays. Given the important roles of kinases in some disease related biological processes, this biosensor shows great potential for a high throughput assay in clinic diagnostics and drug discovery applications.

ACKNOWLEDGMENT

This work was financially supported by the National Natural Science Foundation of China (No. 21005046), National Basic Research Program of China (No. 2007CB310500, No. 2011CB935700), and European Commission Specific Programme GlycoHIT (FP7-HEALTH-2010, No. 260600).

SUPPORTING INFORMATION AVAILABLE

Additional information as noted in text. This material is available free of charge via the Internet at http://pubs.acs.org.

Received for review September 2, 2010. Accepted October 9, 2010.

AC102296G